Asian Journal of Chemistry; Vol. 29, No. 5 (2017), 1098-1102

ASIAN JOURNAL OF CHEMISTRY

https://doi.org/10.14233/ajchem.2017.20429

Electrochemical Determination of Paracetamol Based on Graphene-TiO_2 Modified Glassy Carbon Electrode

T. JYOTHISH KUMAR[1,*], S. RENJINI[2], K. SREEVALSAN[1] and V. ANITHAKUMARY[2]

[1]Department of Chemistry, S.N. College, Kollam-691 001, India
[2]Department of Chemistry, S.N. College for Women, Kollam-691 001, India

*Corresponding author: E-mail: jyothishsree@gmail.com

Received: 30 November 2016; *Accepted*: 27 January 2017; *Published online*: 10 March 2017; AJC-18307

A novel voltametric sensor based on graphene-TiO_2 was developed. The graphene-TiO_2 nanocomposite was prepared by the hydrothermal treatment. It provides an efficient and facile approach to yield nanocomposite with TiO_2 nanoparticles uniformly embedded on graphene substrate. The crystallinity and crystalline size were examined by XRD and TEM. The surface morphology of the nanocomposite is examined by SEM. The crystalline size of the as prepared nanocomposite was 17 nm. The electrochemical behaviour of paracetamol was investigated with this sensor. The graphene-TiO_2 modified electrode exhibited a linear response in differential pulse voltametry, with the detection limit of 11.38×10^{-8} M.

Keywords: Graphene, Paracetamol, Hydrothermal method, Graphene-TiO_2 nanocomposite.

INTRODUCTION

Graphene is a 2D sheet of sp^2 bonded carbon atoms, densely packed in a honeycomb crystal lattice structure whereby each of these layers is held together by weak van der Waals forces [1]. The most important property of graphene is its excellent electrical conductivity. The various forms of graphene-based materials include thermally reduced graphene oxide (TRGO), chemically reduced graphene oxide (CRGO) and electrochemically reduced graphene oxide (ERGO), contains oxygen-containing functional groups and certain amounts of defects [2-4]. The rapid electron transfer takes place at the surface of edge planes and defects when compared to the basal planes for the electrochemical sensors fabricated with graphene based materials [5-7]. The presence of these structural defects in the chemically modified grapheme can be exploited for electrochemical sensor applications. The presence of oxygen-containing functional groups in the graphene-based materials play a vital role in the electrochemical sensors, which makes the adsorption and preconcentration of the redox species and effectively catalyze the redox reactions. In addition, the presence of these functional groups makes an effective functionalization with various biomolecules and polymers for applications [8-10]. The functionalization of these graphene based materials with specific functional groups can enable the use of these excellent materials for electrochemical sensor applications with specific analytes. The functionalized graphene materials also make fast electron transfer by pre-concentrating the target analytes at the electrode surface.

Graphene-based nanocomposites with semiconductor and metal nanoparticles have received increasing attention due to their remarkable electrocatalytic, electrochemical sensing and electrochemical energy conversion properties [11-22]. The remarkable properties of metal nanoparticles incorporated on graphene depicts high electrocatalytic activity, excellent conductivity and selectivity which makes metal nanostructures decorated on graphene an ideal choice to be used as an active material in electrochemical sensors.

Due to its good biocompatibility and high conductivity, TiO_2 has been widely used in the fabrication of electrochemical biosensors [23-29]. In these biosensors, TiO_2 was employed as support matrix for immobilizing enzymes, which can facilitate the direct electron transfer and enhance the catalytic activity of enzymes.

Acetaminophen or paracetamol or N-acetyl *p*-aminophenol or N-(4-hydroxy phenyl) ethanamide is commonly used and extensively established over the counter drugs of the world [30]. Paracetamol has been clinically proven to be highly effective against headache, mascular pain, joint pain and even in the osteoarthritis therapy.

EXPERIMENTAL

Graphite powder (320 mesh, spectrum pure) was purchased from Sinopharm Chemical Reagent Co., Ltd. Titanium

isopropoxide was obtained from Sigma Aldrich. Other chemicals used in this study were of analytical grade. All solutions were prepared with double distilled water. All the prepared samples were analyzed with PXRD, SEM, Cyclic voltammetry (CV) and differential pulse voltammograms (DPVs) were recorded using CHI 604D electrochemical analyzer, in a conventional three-electrode cell. A platinum wire, Ag/AgCl and a glassy carbon electrode (GCE) modified with the composite were used as counter electrode, reference electrode and working electrode, respectively. All experiments were carried out at room temperature.

Preparation of graphene/TiO_2 nanocomposite: Graphene oxide was synthesized from graphite powder by the modified Hummers method [13]. Graphene was prepared by the thermal exfoliation of graphene oxide. Hydrothermal preparation of graphene/TiO_2 nanocomposite was carried out by the following procedure. Titanium isopropoxide (0.2 mL) was mixed with graphene (50 mg) in a 25 mL Teflon-sealed autoclave and H_2SO_4 (1 M, 2 mL) was then added. The resultant mixture was ultrasonicated for 10 min and then the autoclave was kept in oven maintained at 170 °C for 24 h. The final product was isolated by filtration, rinsed thoroughly with deionized water and methanol and dried in vacuum. The graphene/TiO_2 nanocomposite was obtained in the form of black powder.

Preparation of modified electrode: The as prepared graphene-TiO_2 nanaocomposite (1.5 mg) was dispersed in 1 mL DMF to form a homogenous suspension. The graphene-TiO_2 modified glassy carbon electrode was prepared by dropping 7 µL of the suspension on the surface of freshly polished glassy carbon electrode and dried.

RESULTS AND DISCUSSION

Characterization of graphene oxide and reduced graphene oxide: Fig. 1 shows the XRD patterns of graphene oxide prepared by the modified Hummers method [13]. Fig. 2 depicts the XRD pattern of graphene prepared by the thermal exfoliation of graphene oxide.

Characterization of graphene-TiO_2 nano composite: The crystalline phase of TiO_2-graphene nanocomposite was determined by powder X-ray diffraction. As shown in Fig. 3, the XRD patterns can be indexed to the anatase TiO_2 phase

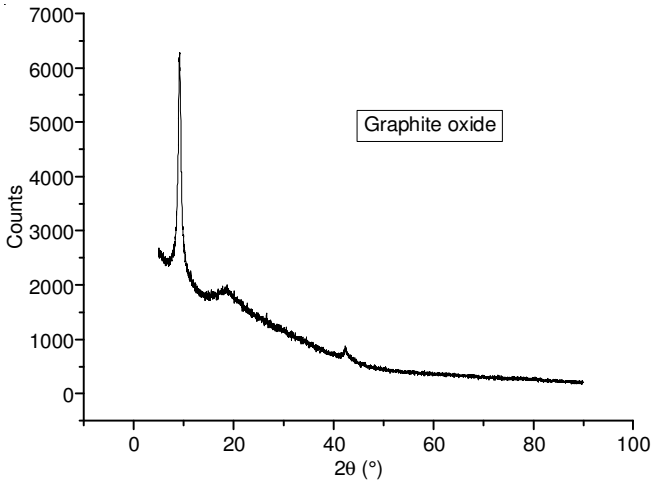

Fig. 1. X-ray diffraction of graphene oxide

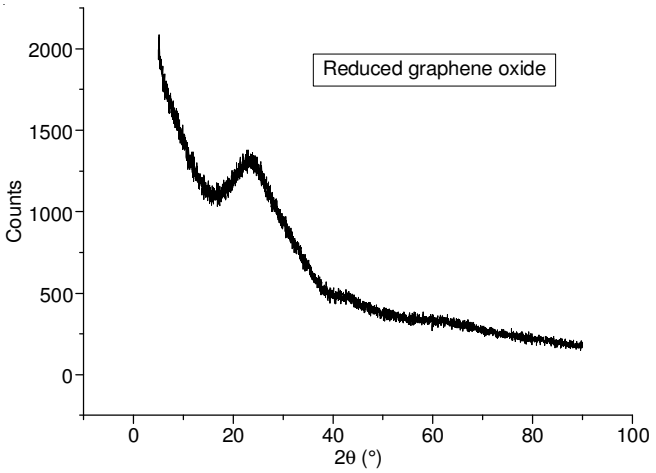

Fig. 2. X-ray diffraction of graphene

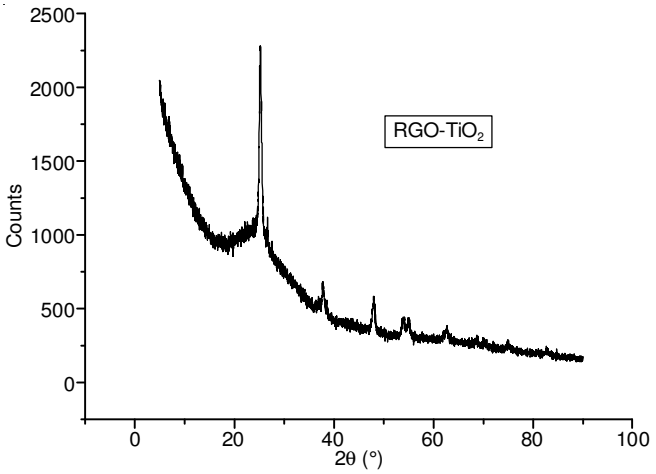

Fig. 3. X-ray diffraction of graphene-TiO_2 nano composite

(JCPDS file no. 89-4921), suggesting the complete formation of anatase TiO_2 during the hydrothermal process. The high intensity and the small width at the half height of the diffraction peaks indicate the big crystallized portion of the TiO_2 particles on the surface of graphene. However, the diffraction peaks of graphene are not distinguishable in XRD patterns of the nanocomposite, which might be ascribed to their low diffraction intensity and shielding of the graphene peaks by those of TiO_2.

The SEM image of TiO_2-graphene is given in Fig. 4. It can be seen that TiO_2 was formed in a highly faceted morphology on the substrates of graphene with about 50-100 nm diameter for the clusters. The structure characterization results suggest that hydrothermal reaction proceeded with efficient crystallization of TiO_2 in anatase phase and their *in situ* immobilization on graphene substrate.

TEM analysis revealed a homogeneous distribution of TiO_2 nano particles at the surface of grapheme shown in Fig. 5. From the images it is observed that the graphene is composed of well dispersed TiO_2 nano particles with dark regions showing partly agglomerated nanoparticles.

Electrochemical response of paracetamol towards modified electrodes: The electrochemical behaviour of paracetamol at bare GCE, graphene/GCE and graphene-TiO_2/GCE was investigated and the results are shown in Fig. 6. The peak

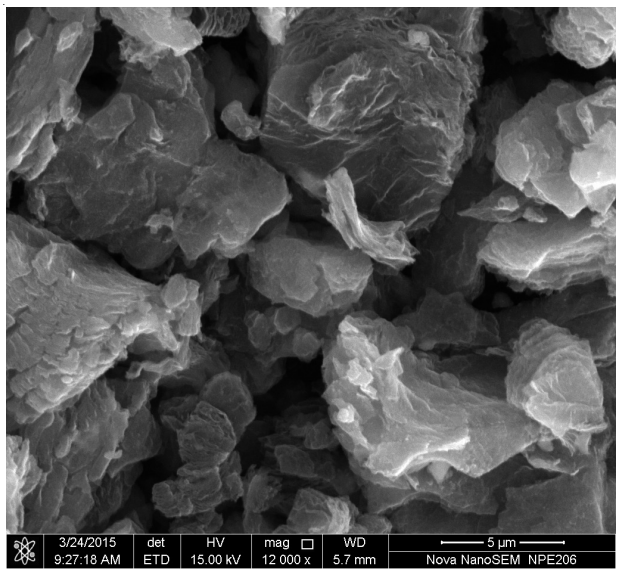

Fig. 4. SEM images of graphene-TiO_2 nano composite

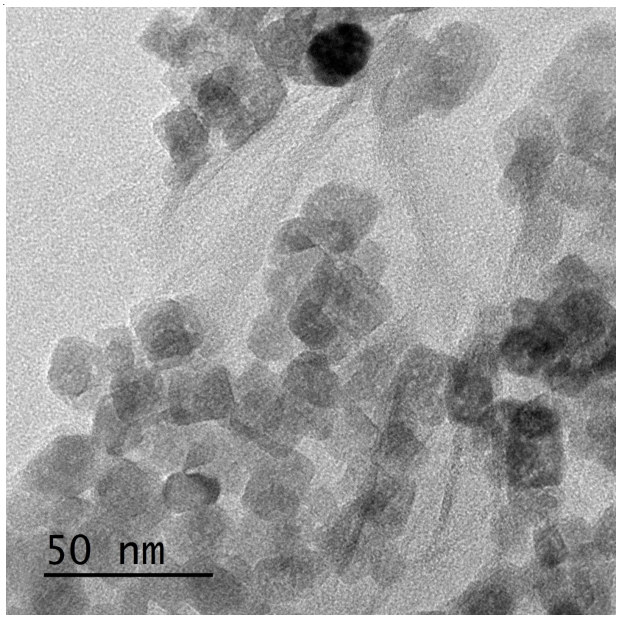

Fig. 5. TEM images of graphene-TiO_2 nanocomposite

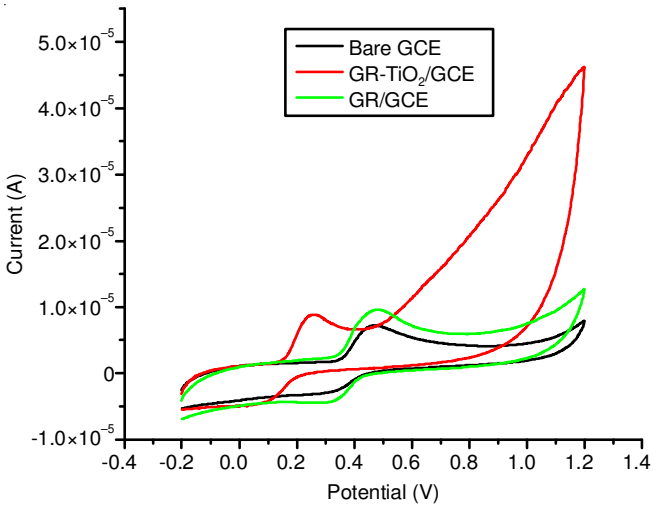

Fig. 6. Cyclic voltammograms of 2 × 10^{-4} M paracetamol at bare GCE, graphene/GCE and graphene-TiO_2/GCE in 0.1 M PBS (pH 7)

potential of graphene-TiO_2/GCE is lower than the peak potential of graphene/GCE. It is shown that a pair of redox peak appears at the typical cyclic voltammetry at graphene-TiO_2/GCE electrodes in the potential range at a scan rate of 100 mV/s are shown in Fig. 6. This suggest the synergistic effect of graphene-TiO_2 nanocomposite provides an efficient micro enivironment for the electrochemical reaction of paracetamol.

Influence of pH on the electrolytic oxidation of paracetamol: Fig. 7 shows the effect of pH on the current response of dopamine on the graphene-TiO_2/GCE electrode. The oxidation peak current gradually increased with increase of pH values from 4 to 6, then the oxidation peak current decreases from 6-8. Therefore considering the sensitivity pH 6 was taken for the subsequent experiments.

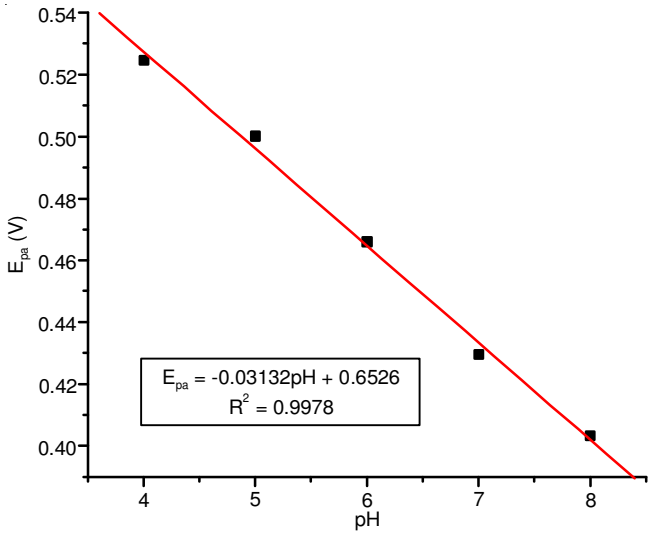

Fig. 7. Cyclic voltammograms of paracetamol at different pH

Effect of scan rate on the detection of paracetamol at modified electrode: To further investigate the electrochemical kinetics at the composite electrode, cyclic voltammetry was recorded at various scan rates. Both anodic and cathodic peak currents increase with scan rate. The voltametric peak currents increases with increase of square root of scan rate, *i.e.* peak current proportional to $v^{1/2}$ indicates that the electron transfer at the electrode is controlled by diffusion which is ideal condition for a qualitative analysis and peak appears begins to increase with increase in scan rate indicating a quazi reversible reaction.

Fig. 8(a) sows the cyclic voltammetric curves with scan rates of 10, 100, 200, 300, 400, 500, 600, 700, 800, 900 and 1000 mV/s resp. The oxidation peak current increased gradually with the scan rate. Fig. 8(b) shows the linearity obtained for the relation between redox peak currents and the square root of scan rate.It shows a linear range from 10 to 1000 mV/s with a correlation of 0.9956. This indicates the redox reaction of paracetamol exihibit a diffusion controlled nature at TiO_2-graphene/GCE. To get information about the rate determining step, the Tafel plot was drawn [Fig. 8(c)]. From the equation: E_{pa} = 2.303RT/2(1-a)nF log v + constant, if the value of the electron transfer coefficient (a) was assumed to be equal to 0.5, then n was equal to be 3.20 [30].

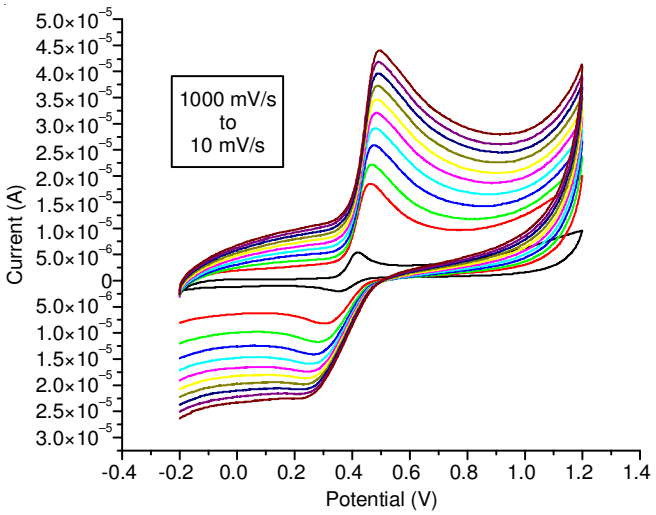

Fig. 8a. Variation of peak current of paracetamol with different scan rates from 10 to 1000 mV/s

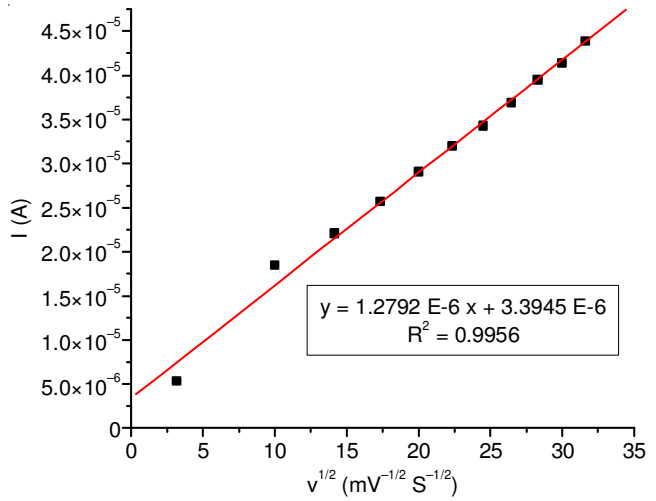

Fig. 8b. Variation of peak current of paracetamol with square root of scan rates from 10 to 1000 mV/s

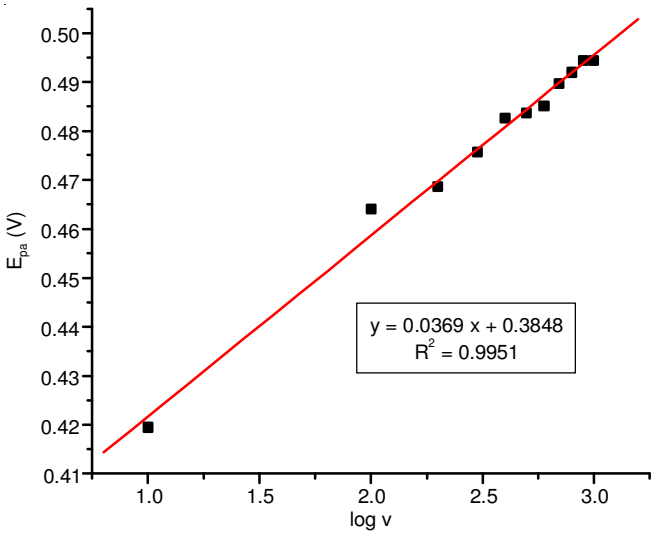

Fig. 8c. Tafel plot

Selective detection paracetamol using graphene-TiO_2/GCE electrode: Differential pulse voltammetry technique was used for the selective detection of paracetamol at graphene-TiO_2/GCE electrode. The results shows a linear relationship between peak currents and paracetamol concentrations within the range from 4×10^{-7} to 2.2×10^{-7} mol/L with a correlation coefficient of 0.9901 and the detection limit was obtained as 11.38×10^{-8} M (Fig. 9).

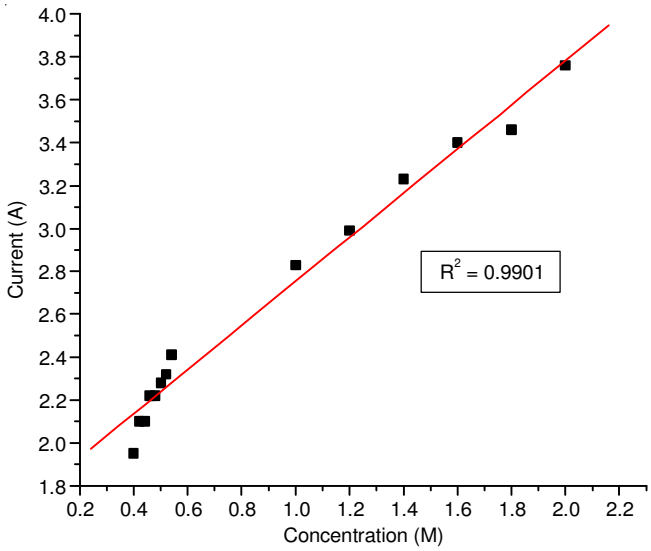

Fig. 9. Differential pulse voltammogram of paracetamol at different concentrations

Conclusion

An electrochemical sensor graphene-TiO_2 modified electrode was prepared for the detection of paracetamol. We successfully synthesized the graphene-TiO_2 nanocomposite by the hydrothermal treatment. The crystallinity and crystalline size were examined by XRD and TEM. The surface morphology of the nanocomposite is examined by SEM. The crystalline size of the as prepared nanocomposite was 17 nm. The sensor exhibited good sensitivity of paracetamol with the detection limit of 11.38×10^{-8} M by differential pulse voltammogram.

ACKNOWLEDGEMENTS

The authors acknowledge Department of Chemistry, Sree Narayana College for Women, Kollam, India for providing the research facilities. The authors also acknowledge to SAIF, Cochin and IISER, Thiruvananthapuram, India for analysis.

REFERENCES

1. W. Choi, I. Lahiri, R. Seelaboyina and Y.S. Kang, *Crit. Rev. Solid State Mater. Sci.*, **35**, 52 (2010); https://doi.org/10.1080/10408430903505036.
2. D.K. Kampouris and C.E. Banks, *Chem. Commun.*, **46**, 8986 (2010); https://doi.org/10.1039/c0cc02860f.
3. S. Wu, Q. He, C. Tan, Y. Wang and H. Zhang, *Small*, **9**, 1160 (2013); https://doi.org/10.1002/smll.201202896.
4. A. Ambrosi, C.K. Chua, A. Bonanni and M. Pumera, *Chem. Rev.*, **114**, 7150 (2014); https://doi.org/10.1021/cr500023c.
5. W. Yuan, Y. Zhou, Y. Li, C. Li, H. Peng, J. Zhang, Z. Liu, L. Dai and G. Shi, *Sci. Rep.*, **3**, 2248 (2013); https://doi.org/10.1038/srep02248.
6. D.A. Brownson, L.J. Munro, D.K. Kampouris and C.E. Banks, *RSC Adv.*, **1**, 978 (2011); https://doi.org/10.1039/c1ra00393c.
7. D.A. Brownson, C.W. Foster and C.E. Banks, *Analyst*, **137**, 1815 (2012); https://doi.org/10.1039/c2an16279b.

8. M. Pumera, *Chem. Soc. Rev.*, **39**, 4146 (2010); https://doi.org/10.1039/c002690p.
9. X. Chen, G. Wu, Y. Jiang, Y. Wang and X. Chen, *Analyst*, **136**, 4631 (2011); https://doi.org/10.1039/c1an15661f.
10. M. Zhou, Y. Zhai and S. Dong, *Anal. Chem.*, **81**, 5603 (2009); https://doi.org/10.1021/ac900136z.
11. P.V. Kamat, *J. Phys. Chem. Lett.*, **1**, 520 (2010); https://doi.org/10.1021/jz900265j.
12. D. Chen, L. Tang and J. Li, *Chem. Soc. Rev.*, **39**, 3157 (2010); https://doi.org/10.1039/b923596e.
13. M. Pumera, *Chem. Soc. Rev.*, **39**, 4146 (2010); https://doi.org/10.1039/c002690p.
14. Y. Shao, S. Zhang, C. Wang, Z. Nie, J. Liu, Y. Wang and Y. Lin, *J. Power Sources*, **195**, 4600 (2010); https://doi.org/10.1016/j.jpowsour.2010.02.044.
15. H. Zhang, X. Lv, Y. Li, Y. Wang and J. Li, *ACS Nano*, **4**, 380 (2010); https://doi.org/10.1021/nn901221k.
16. L. Dong, R.R.S. Gari, Z. Li, M.M. Craig and S. Hou, *Carbon*, **48**, 781 (2010); https://doi.org/10.1016/j.carbon.2009.10.027.
17. S. Guo, D. Wen, Y. Zhai, S. Dong and E. Wang, *ACS Nano*, **4**, 3959 (2010); https://doi.org/10.1021/nn100852h.
18. C. Shan, H. Yang, D. Han, Q. Zhang, A. Ivaska and L. Niu, *Biosens. Bioelectron.*, **25**, 1070 (2010); https://doi.org/10.1016/j.bios.2009.09.024.
19. Y. Li, L. Tang and J. Li, *Electrochem. Commun.*, **11**, 846 (2009); https://doi.org/10.1016/j.elecom.2009.02.009.
20. Y. Zhang, H. Li, L. Pan, T. Lu and Z. Sun, *J. Electroanal. Chem.*, **634**, 68 (2009); https://doi.org/10.1016/j.jelechem.2009.07.010.
21. D. Wang, D. Choi, J. Li, Z. Yang, Z. Nie, R. Kou, D. Hu, C. Wang, L.V. Saraf, J. Zhang, I.A. Aksay and J. Liu, *ACS Nano*, **3**, 907 (2009); https://doi.org/10.1021/nn900150y.
22. K. Wang, Q. Liu, X.Y. Wu, Q.M. Guan and H.N. Li, *Talanta*, **82**, 372 (2010); https://doi.org/10.1016/j.talanta.2010.04.054.
23. E. Topoglidis, C.J. Campbell, A.E.G. Cass and J.R. Durrant, *Langmuir*, **17**, 7899 (2001); https://doi.org/10.1021/la010309b.
24. S. Liu and A. Chen, *Langmuir*, **21**, 8409 (2005); https://doi.org/10.1021/la050875x.
25. A. Liu, M. Wei, I. Honma and H. Zhou, *Adv. Funct. Mater.*, **16**, 371 (2006); https://doi.org/10.1002/adfm.200500202.
26. S.J. Bao, C.M. Li, J.F. Zang, X.Q. Cui, Y. Qiao and J. Guo, *Adv. Funct. Mater.*, **18**, 591 (2008); https://doi.org/10.1002/adfm.200700728.
27. Y. Luo, H. Liu, Q. Rui and Y. Tian, *Anal. Chem.*, **81**, 3035 (2009); https://doi.org/10.1021/ac802721x.
28. H. Lin, X. Ji, Q. Chen, Y. Zhou, C.E. Banks and K. Wu, *Electrochem. Commun.*, **11**, 1990 (2009); https://doi.org/10.1016/j.elecom.2009.08.034.
29. Y. Luo, Y. Tian, A. Zhu, Q. Rui and H. Liu, *Electrochem. Commun.*, **11**, 174 (2009); https://doi.org/10.1016/j.elecom.2008.10.056.
30. N.F. Atta, A. Galal, F.M. Abu-Attia and S.M. Azab, *J. Mater. Chem.*, **21**, 13015 (2011); https://doi.org/10.1039/c1jm11795e.